 ©2011 Kvantovaya Elektronika and Turpion Ltd

PACS numbers: 42.55.Wd; 42.60.By; 42.60.Da; 42.60.Jf
DOI: 10.1070/QE2011v041n12ABEH014617

Coherent beam combining of pulsed fibre amplifiers with active phase control*

X.L. Wang, P. Zhou, Y.X. Ma, H.T. Ma, X.J. Xu, Z.J. Liu, Y.J. Zhao

Abstract. **Coherent beam combining of pulsed fibre lasers is a promising method for power scaling while simultaneously maintaining good beam quality. We propose and demonstrate a scalable architecture for coherent beam combining of all-fibre pulsed amplifiers with active phase control using the stochastic parallel gradient descent (SPGD) algorithm. A low-pass filter is introduced to eliminate the fluctuation of the metric function caused by pulsed lasers and to extract the exact phase noise signal. Active control is thereby based on the SPGD algorithm, resulting in stable coherent beam combining at the receiving plane even in a turbulent environment. Experimental results show that the fringe visibility of the long exposure pattern increases from 0 to 0.4, and the power encircled in the main-lobe increases by 1.6 times when the system evolves from the open-loop phase-locking scheme to the closed-loop scheme. This architecture can be easily scaled up to a higher power by increasing the number of amplifying channels and the power of a single amplifier.**

Keywords: *active phase control, pulsed fibre amplifiers, coherent beam combining.*

1. Introduction

High-peak-power pulsed fibre lasers are widely used in many applications including remote sensing, material processing, nonlinear frequency generation, long-range energy delivery, etc. However, thermal load, fibre damage and nonlinear effects [1] hinder the achievement of an ultimate peak power with the help of a single fibre laser. Coherent beam combining of pulsed fibre lasers is an alternative way for power scaling while simultaneously maintaining good beam quality [2]. In previous work, coherent beam combining of pulsed lasers – including a *Q*-switched multi-core photonic crystal fibre laser [3], an external resonator with diffraction coupling and spatial filtering [4], a self-Fourier external cavity [5] – involved passive phasing. Although phase locking of a pulsed fibre amplifier with a continuous wave (cw) seed laser by sensing the phase of a low optical leakage between pulses using a heterodyne phase detection technique was implemented in [6], to the best of our knowledge, coherent beam combining of two or more pulsed fibre amplifier arrays with active phase control has not yet been demonstrated.

In this paper, we demonstrate a scalable architecture for coherent beam combining of all-fibre pulsed amplifiers with active phase control using the stochastic parallel gradient descent (SPGD) algorithm. A low-pass filter is introduced to eliminate the fluctuation of the metric function caused by pulsed lasers and to extract the exact phase noise signal for the SPGD-algorithm-based active phase control. Active control is thereby built, resulting in stable coherent beam combining at the receiving plane even in a turbulent environment. The fringe visibility of the long exposure pattern increases from 0 two 0.4 and the power encircled in the main-lobe is 1.6-times higher when the system evolves from the open-loop scheme to the closed-loop scheme. This architecture can be easily scaled up to a higher power by increasing the number of amplifying channels and the power of single amplifier, which makes scalable high-power coherent beam combining of pulsed lasers quite promising.

2. Theoretical analysis and numerical simulation

2.1. Theoretical analysis of coherent combining of pulsed fibre lasers

There are three main methods including heterodyne phase detection techniques [7–9], a multi-dithering technique [10–13], and an optimal algorithm [14–16] (especially, the SPGD algorithm) for active phase control in active phasing and coherent beam combining. With such advantages as few components, model- and phase-free detection, the method of coherent beam combining based on the SPGD algorithm makes the system compact. The method has been proposed to build a new architecture of high-energy laser systems. Moreover, the SPGD algorithm is a potential technique for coherent beam combining of pulsed fibre lasers.

In coherent beam combining of cw lasers, the steps of the SPGD algorithm can be briefly described as follows. The metric function J is usually defined as the power in the main lobe of the interference pattern encircled in a pinhole, which is detected by a photodetector [15, 17, 18]. In this case, $J = J(u_1, u_2, \ldots, u_N)$, where u are the control signals applied to phase modulators, N is the channel number of lasers/amplifiers to be combined. The algorithm is implemented in infinite iterations and can be terminated manually. Each iteration cycle works as follows.

(1) Statistically independent random perturbations δu_1, δu_2, …, δu_N (where all $|\delta u_i|$ are small values) are generated; they are typically chosen as statistically independent variables having a zero mean and equal variances: $\langle \delta u_k \rangle = 0$, $\langle \delta u_k \delta u_1 \rangle = \sigma^2 \delta_{kl}$, where δ_{kl} is the Kronecker symbol.

(2) Control voltages with the positive perturbations are applied and the metric function is obtained from the detector,

* Reported at the Conference 'Laser Optics 2010', Russia, St. Petersburg.

X.L.Wang, P.Zhou, Y.X.Ma, H.T.Ma, X.J.Xu, Z.J.Liu, Y.J.Zhao
College of Optoelectronic Science and Engineering, National University of Defense Technology, Changsha, Hunan, 410073, China; e-mail: chinawxllin@163.com

Received 25 February 2011
Kvantovaya Elektronika **41** (12) 1087–1092 (2011)
Submitted in English

$J^+ = J(u_1 + \delta u_1, u_2 + \delta u_2, \ldots, u_N + \delta u_N)$. Then, control voltages with the negative perturbations are applied and the metric function, $J^- = J(u_1 - \delta u_1, u_2 - \delta u_2, \ldots, u_N - \delta u_N)$, is obtained.

(3) Difference between two evaluations of the metric function is calculated: $\delta J = J^+ - J^-$.

(4) Control voltages are updated: $u_i = u_i + \gamma \delta u_i \delta J$, $i = 1, 2, \ldots, N$, where γ is the update gain ($\gamma > 0$ corresponds to the procedure of maximization and $\gamma < 0$ – to that of minimization).

In coherent beam combining using the SPGD algorithm, the metric function J is a function of the phase $(\varphi_1, \varphi_2, \ldots, \varphi_N)$ of each laser for the control signals, which depend not only on the phase noise but also on the control signals themselves. Furthermore, control signals generated by the SPGD algorithm are determined by the metric function J. Thus, to obtain an accurate metric function is the key point for the active phase control of the SPGD algorithm. Taking into account the fact that the metric function is usually defined as the power in the main lobe of the interference pattern encircled in a pinhole, the fluctuation of the metric function is only caused by the phase noise of each laser. Hence, the metric function maximization establishes phase locking of each laser in coherent beam combining of cw lasers. But in coherent beam combining of pulsed fibre lasers, the periodically changing metric function contains not only the phase noise of each laser, but also the fluctuation of the laser intensity. Thus, using the metric function for active phase control is not feasible for phase locking. If the fluctuation of the metric function caused by the use of pulsed lasers can be eliminated and the exact phase noise signal can be extracted, this corrected metric function can be used for phase locking.

To eliminate the fluctuation of the metric function caused by the use of pulsed lasers and to extract the exact phase noise signal, use can be made of a low-pass filter. Taking into account the fact that the phase noise frequency of the fibre amplifier is almost 100 Hz, the variance at the phase noise frequencies above 1 kHz is less than $\lambda/30$, and most pulsed lasers have a repetition rate higher than 10 kHz, a low-pass filter with a 3-dB cut-off frequency of 3 to 5 kHz is effective to eliminate the pulsed laser intensity fluctuations and to extract the exact phase noise signal from the metric function. Thus, active phase control can be established using the corrected metric (which only contains information about the phase noise and is almost the same as the metric function) and the SPGD algorithm.

Another key point for coherent beam combining is the synchronisation of each laser. In most cases, the delay line may be necessary for accurate synchronisation control of each laser.

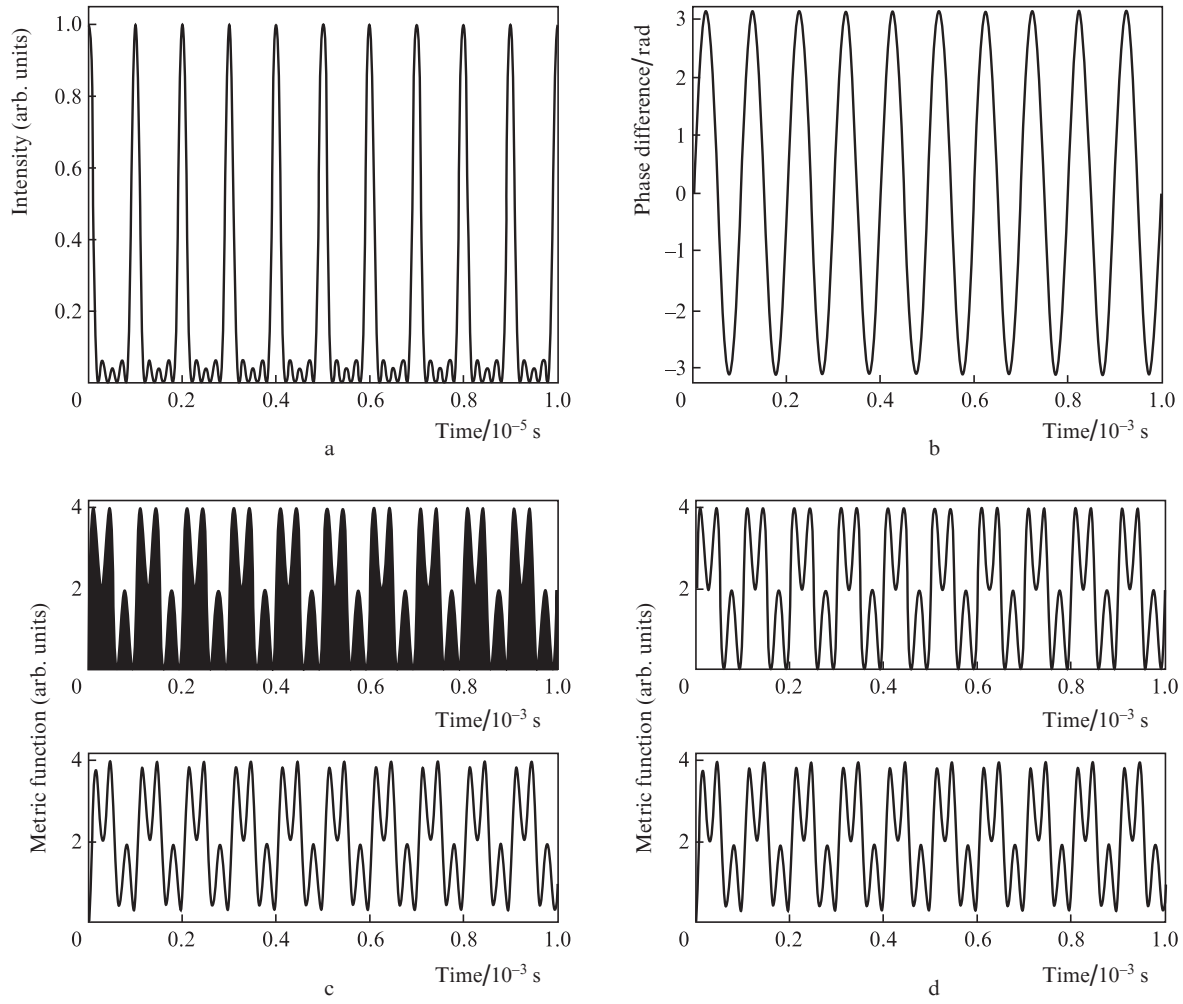

Figure 1. Simulation results of coherent beam combining of mode-locked pulsed lasers with a sine-wave phase noise. (a) Waveform of the pulsed laser, (b) waveform of phase noise, (c) metric function before (top) and after (bottom) the low-pass filter, (d) metric function of cw lasers (top) and metric function of pulsed lasers (bottom) after the low-pass filter.

2.2. Numerical simulation

The feasibility of the low-pass filter for eliminating the metric function fluctuations caused by the use of pulsed lasers and for extracting the exact phase noise signal is simulated numerically. In simulation, we consider the simplest case, namely, the coherent beam combining of two lasers only. The first laser is a mode-locked pulsed laser with a repetition rate of 1 MHz and a sine-wave phase noise with a frequency of 10 kHz. The second one is a sine-wave pulsed laser with a pulse repetition rate of 1 MHz. In this case, the white phase noise with an amplitude of 0.5 and a sample rate of 10 kHz is used as a model noise in the simulation.

Taking into account the fact that the repetition rate of the each pulsed laser is 1MHz, and the frequency of the phase noise is 10 kHz, a low pass filter with a cut-off frequency of about 100 kHz is used to eliminate the metric function fluctuations caused by the use of pulsed lasers.

Figure 1 present the simulation results of the coherent beam combining of mode-locked fibre lasers with a sine-wave phase noise. Figures 1a and b show the waveforms of the pulsed laser and the phase noise, respectively. Figure 1c illustrates the metric functions upon coherent beam combining of pulsed lasers before and after the low-pass filter. Figure 1d shows the metric function upon coherent beam combining of a cw laser and the metric function upon coherent beam combining of pulsed lasers after the low-pass filter. One can see from Fig. 1d that the relative coefficient between the metric function upon coherent beam combining of a cw laser and upon coherent beam combining of pulsed lasers with a low-pass filter is 0.94, which indicates that the low-pass filter can eliminate the metric function fluctuations, caused by the use of pulsed lasers, and extract the exact phase noise signal.

Figure 2 shows the simulation results of coherent combining of two lasers with a white noise phase difference and a sine-wave waveform. As in Fig. 1, the relative coefficient between the metric function upon coherent beam combining of a cw laser and coherent beam combining of pulsed lasers with a low-pass filter is 0.99, which also indicates that the low-pass filter can eliminate the metric function fluctuation, caused by the use of pulsed lasers, and extract the exact phase noise signal.

3. Experimental results and discussions

The experimental setup is shown in Fig. 3. A single frequency fibre laser (central wavelength, 1064.3 nm; linewidth, < 50 kHz; power, > 10 mW) is intensity modulated by an intensity

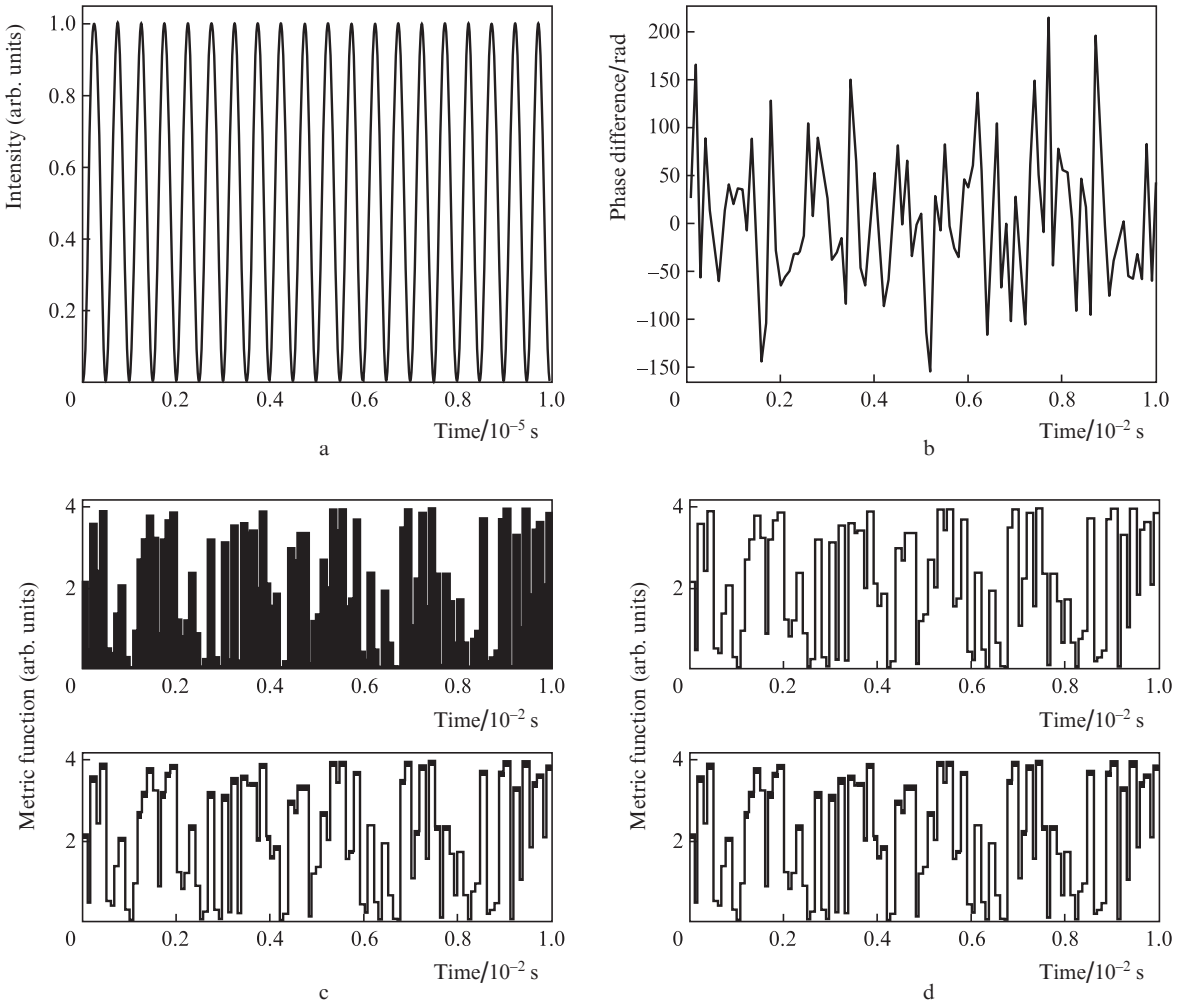

Figure 2. Simulation results of coherent combining of a sine-wave laser with a white noise phase. (a) Waveform of the pulsed laser, (b) waveform of the phase noise, (c) metric function before (top) and after (bottom) the low-pass filter, (d) metric function of cw lasers (top) and metric function of pulsed lasers (bottom) after the low-pass filter.

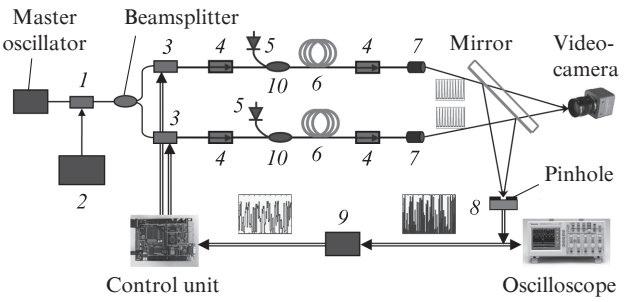

Figure 3. Experimental setup of coherent beam combining of pulsed fibre amplifiers: (*1*) intensity modulator; (*2*) function generator; (*3*) phase modulator; (*4*) isolator; (*5*) laser diode; (*6*) YB^{3+}-doped fibre; (*7*) collimator; (*8*) photodetector; (*9*) loss-pass filter; (*10*) wavelength division multiplexer.

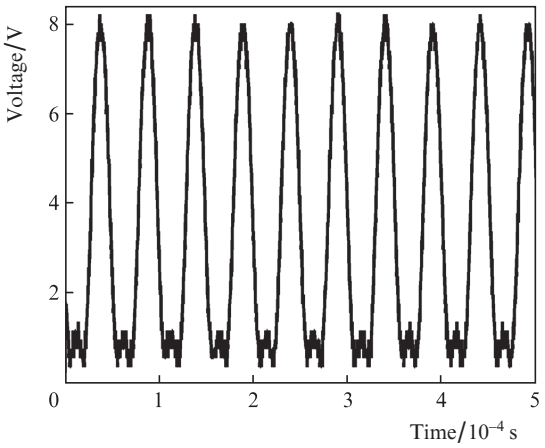

Figure 4. Intensity of the pulsed laser.

modulator with a sine-wave waveform generated by the function generator, which corresponds to generation of a pulsed fibre laser. The pulsed laser beam is split into two beams. Each beam passes through a phase modulator and an isolator, and then propagates to a home-made fibre amplifier to scale the mean power up to 100 mW. In each amplifier, a 1.5-m-long Yb^{3+}-doped fibre is pumped by a laser diode through a wavelength division multiplexer. The output amplified laser beam is isolated by an isolator, and then collimated by a collimator. The tilt angle of the laser beams is carefully tuned to ensure the laser beams overlap with each other at the observion plane of the camera. The collimated output beam array is sampled by a mirror. After the sampler, the reflected part of the beam is directed to a home-made pinhole with a radius of 50 μm. A photodetector is located behind the pinhole. The location of the pinhole is carefully adjusted to ensure the maximum output signal of the detector. The optical power detected with the photoelectric detector passing through the low-pass filter is defined as the weight function J and is used in the SPGD algorithm. Another part of the beam after the sampler is

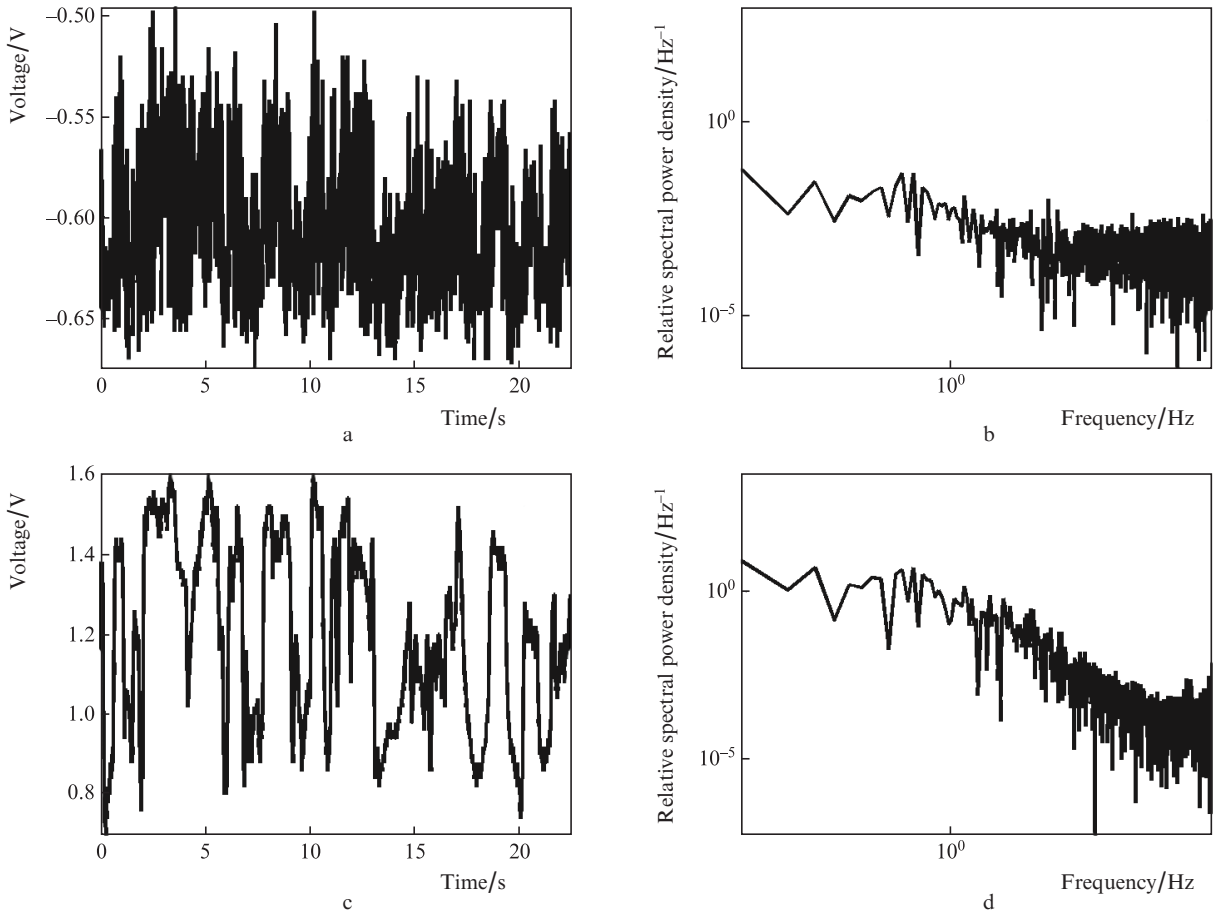

Figure 5. (a, c) Time-domain and (b, d) frequency-domain characteristics of the metric function (a, b) before and (c, d) after the low-pass filter.

directed to an IR camera to diagnose the profile of the combined beam. In our experiment, the SPGD algorithm is performed on a digital signal processor, whereas phase control signals are sent to the phase modulators through digital-to-analogue converters.

Firstly, pulsed laser radiation is generated when the intensity modulator modulates a 20-kHz sine-wave signal. As follows from Fig. 4, the pulse repetition rate is 20 kHz and the pulse duration is about 20 μs. Without the delay line, the optic path difference is also easily controlled to be 0.1 m by controlling the fibre length in the amplifier via cutting and splicing the fibre. Thus, the pulse synchronisation error is controlled to be less than 0.0017%, which is small enough and can be neglected.

To eliminate the metric function fluctuations caused by the use of pulsed lasers, we designed a simple RC low-pass filter. Use was made of a 1-kΩ resistor and a 1-μF capacitor. The cut-off frequency at the 3-dB level was about 1 kHz. The metric functions before and after the low-pass filter were investigated experimentally. Figure 5 shows both characteristics in time domain and frequency domain. One can see that the designed low-pass filter makes it possible to eliminate the metric function fluctuations caused by the use of pulsed lasers and to extract the exact phase noise signal, thereby implementing the active phase control. The experiment demonstrated in-phase locking (phase difference between the beams of two lasers was $2n\pi$) and out-of-phase locking (phase difference between the beams of two lasers was $2n\pi + \pi$). In the case of out-of-phase locking, we have $\gamma < 0$ during step (4) of the iteration function, whereas in the case of in-phase locking, we have $\gamma > 0$.

Results of the experiment are shown in Fig. 6. The curve shows the evolution of the metric function (before the low-pass filter) from out-of-phase locking to open-loop (without phase locking) and then to in-phase locking, corresponding to long exposure interference patterns. In the open-loop scheme, the mean value of the metric function is 19.4 mV, and the visibility of long exposure interference patterns is zero. After setting $\sigma = 0.1$ and $\gamma = -0.3$ in the SPGD algorithm, the out-of-phase locking is established. The metric function (mean value is 13.7 mV) in the out-of-phase scheme is 0.7 times of the value in the open-loop scheme. The visibility of the corresponding long exposure out-of-phase interference pattern is 0.41. After setting $\sigma = 0.1$ and $\gamma = 0.3$ in the SPGD algorithm, in-phase locking is established. The metric function in the in-phase scheme is 1.61 times of the value in the open-loop scheme, and the fringe visibility increases from 0 to 0.33. Here, the visibility is defined by the formula $(I_{max} - I_{min})/(I_{max} + I_{min})$, where I_{max} and I_{min} are the intensities in the maximum and adjacent minimum of the interference pattern, respectively.

Although the mean power of laser radiation is low in our experiment, the used architecture can be easily scaled up to a higher power by increasing the number of amplifying channels and the power of a single amplifier, which makes scalable high-power coherent beam combining of pulsed lasers quite promising.

4. Conclusions

The paper offers and demonstrates a scalable architecture for coherent beam combining of all-fibre pulsed amplifiers with active phase control using the SPGD algorithm. The key point is the use of a low-pass filter to convert the pulsed radiation to the cw radiation. A 1-kHz low-pass filter is introduced to eliminate the metric function fluctuations caused by the use of pulsed lasers and to extract the exact phase noise signal. Active control is thereby built on the SPGD algorithm, and stable coherent beam combining can be obtained at the receiving plane even in a turbulent environment. Experimental results shows the fringe visibility of the long exposure pattern increases from 0 to 0.4 and the power encircled in the main-lobe increases by 1.6 times when the system evolves from the open-loop scheme to the closed-loop in-phase locking scheme. There are three points we should take into account in this architecture. First, the pulse repetition rate of a pulsed fibre laser should be much higher than the phase noise. Second, accurate synchronisation of each pulsed laser is need. And

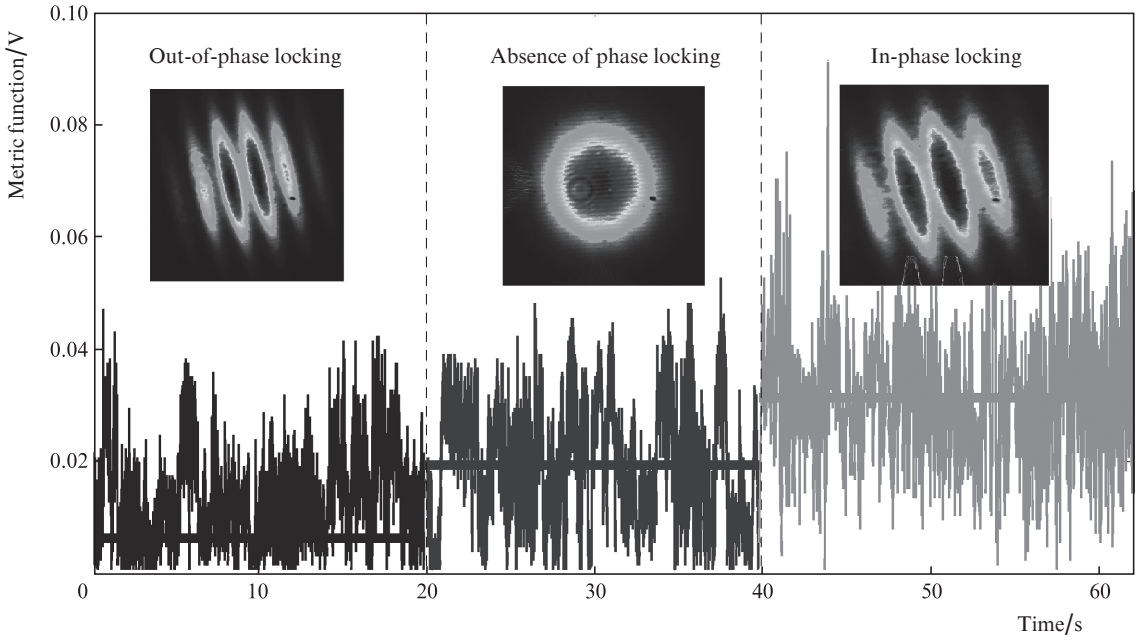

Figure 6. Experimental results of phase locking.

finally, careful selection of the low-pass filter parameters is important to extract the exact phase noise signal for the SPGD-algorithm-based active phase control. Although the mean power is low in our experiment, the architecture can be easily scaled up to a higher power by increasing the number of amplifying channels and the power of a single amplifier, which makes scalable high-power coherent beam combining of pulsed lasers quite promising.

Acknowledgements. This work is supported by the Innovation Foundation for Graduates of the National University of Defense Technology, China (Grant No. B080702).

References

1. Galvanauskas A. *Opt. Photon. News*, **15**, 42 (2004).
2. Jeong Y., Sahu J.K., Payne D.N., Nilsson J. *Opt.Express*, **12**, 6088 (2004).
3. Michaille L., Taylor D.M., Bennett C.R., Shepherd T.J., Ward B.G. *Opt. Lett.*, **33**, 4200 (2008).
4. Kong F., Liu L., Sanders C., Chen Y.C., Lee K.K. *Appl. Phys. Lett*., **90**, 151110 (2007).
5. Corcoarn C.J., Durville F. *Appl. Phys. Lett*., **86**, 20118 (2005).
6. Cheung E.C., Weber M., Rice R.R. *Phase Locking of a Pulsed Fiber Amplifier* (Japan, 2008) paper WA2.
7. Goodno G.D., Komine H., McNaught S.J., Weiss S.B., Redmond S., Long W., Simpson R., Cheung E.C., Howland D., Epp P., Weber M., McClellan M., Sollee J., Injeyan H. *Opt. Lett*., **31**, 1247 (2006).
8. Goodno G.D., Asman C.P., Anderegg J., Brosnan S., Cheung E.C., Hammo D., Injeyan H., Komine H., Long W.H., McClellan M., Jr, McNau S.J., Redmond S., Simpson R., Sollee J., Weber M., Weiss S.B., Wickham M. *IEEE J. Sel. Top. Quantum Electron.*, **13**, 460 (2007).
9. Augst S.J., Fan T.Y., Sanchez A. *Opt. Lett.*, **29**, 474 (2004).
10. Shay T.M. *Opt. Express*, **14**, 12188 (2006).
11. Shay T.M., Benham V., Baker J.T., Ward B., Sanchez A.D., Culpepper M.A., Pilkington S.D., Spring J., Nelson, D.J., Lu C.A. *Opt. Express*, **14**, 12015 (2006).
12. Jolivet V., Bourdon P., Bennai B., Lombard L., Goular D., Pourtal E., Canat G., Jaouen Y., Moreau B., Vasseur O. *IEEE J. Sel. Top. Quantum Electron.*, **15**, 257 (2009).
13. Ma Y., Zhou P., Wang X., Ma H., Xu X., Si L., Liu Z., Zhao Y. *Opt. Lett*., **35**, 1308 (2010).
14. Vorontsov M.A., Kolosov V. *J. Opt. Soc. Am. A*, **22**, 126 (2005).
15. Zhou P., Ma Y., Wang X., Ma H., Xu X., Liu Z. *Opt. Lett.*, **34**, 2939 (2009).
16. Vorontsov M.A., Weyrauch T., Beresnev L.A., Carhart G.W., Liu L., Aschenbach K. *IEEE J. Sel. Top. Quantum Electron.*, **15**, 269 (2009).
17. Zhou P., Liu Z., Wang X., Yanxing M., Haotong M., Xu X. *Appl. Phys. Lett*., **94**, 231106 (2009).
18. Zhou P., Wang X., Ma Y., Ma H., Liu Z. *Opt. Lett.*, **35**, 950 (2010).